World Electric Vehicle Journal

MDPI

*Article*

# Analysis and Optimization of Fatigue Caused by Vibrations in the Quick-Replacement Battery Box for Electric Vehicles

**Jianying Li [1,*], Guifeng Hu [1] and Junjie Chen [2]**

[1] School of Mechanical and Automotive Engineering, Zhaoqing University, Zhaoqing 526061, China; hgf1203724703@163.com
[2] School of Mechanical and Electrical Engineering, Jiangxi University of Science and Technology, Ganzhou 341000, China; chenjunjie@jxust.edu.cn
* Correspondence: lijianying@zqu.edu.cn

**Abstract:** Quick-replacement battery technology has the advantages of eliminating mileage issues, extending battery life and reducing cost. The battery box plays an important role in carrying and protecting the on-board battery pack. However, fatigue life has not been well-established in changeable operating environments and driving conditions; hence, this knowledge gap is the focus of this paper. Here, SolidWorks (SolidWorks, Waltham, MA, USA) was used to establish a three-dimensional model of a quick-replacement battery box for electric vehicles, OptiStruct software (Altair, Detroit, MI, USA) was used for sweep frequency and random vibration analyses, and random vibration fatigue analysis was carried out using Ncode software (ANSYS, Pittsburgh, PA, USA). The quick-replacement battery box structure was then optimized according to the analysis results and lightweight targets. The results of sweep frequency and random vibration analyses showed that the maximum stress of a quick-replacement battery box is 39.058 Mpa. Compared with the allowable stress of the DC01 material at 150 Mpa, a significant margin is still present. The results of random vibration fatigue analysis showed that the minimum service life of a quick-replacement battery box is $5.740 \times 10^{10}$, which meets the design requirements. Following optimization design, the maximum stress of a quick-replacement battery box was 71.197 Mpa, still meeting the allowable stress of the DC01 material at 150 Mpa and effectively alleviating the stress concentration. Furthermore, the optimized quick-replacement battery box was approximately 4 kg lighter. Therefore, optimization of the quick-replacement battery box is feasible and necessary. The results provide great theoretical and engineering significance for the design and optimization of quick-replacement battery boxes for electric vehicles.

**Keywords:** quick-replacement battery box; finite-element analysis; lightweight design; random vibration fatigue analysis; strength

check for updates

**Citation:** Li, J.; Hu, G.; Chen, J. Analysis and Optimization of Fatigue Caused by Vibrations in the Quick-Replacement Battery Box for Electric Vehicles. *World Electr. Veh. J.* **2023**, *14*, 226. https://doi.org/10.3390/wevj14080226

Academic Editor: Joeri Van Mierlo

Received: 10 July 2023
Revised: 9 August 2023
Accepted: 11 August 2023
Published: 18 August 2023

**Copyright:** © 2023 by the authors. Licensee MDPI, Basel, Switzerland. This article is an open access article distributed under the terms and conditions of the Creative Commons Attribution (CC BY) license (https://creativecommons.org/licenses/by/4.0/).

## 1. Introduction

New energy vehicles have been undergoing rapid developments in recent years [1]. Pure electric vehicles are the primary direction in the development of these types of vehicles, positioning the on-board battery as an energy storage and supply device. Therefore, on-board batteries have become an important component affecting the power, safety, endurance and overall performance of new energy vehicles. The energy supply problem is a key factor that limits the performance of on-board batteries [2]. However, it is not realistic to only focus on charging technologies for on-board batteries. Industry and academia have proposed replacement battery models that make electric vehicles as safe, convenient and fast as traditional refueling vehicles [3]. As a mode of replacement battery, one of the main components of quick-replacement battery technology is the battery box, which carries and protects the on-board battery pack. Therefore, a quick-replacement battery box for electric vehicles has increasingly attracted the attention of scholars.

Lu et al. [4] used mode analysis to study the structure of the quick-replacement battery boxes for electric vehicles, and analyzed it under free and constraint modes. Wang et al. [5] evaluated the structural strength and stiffness of quick-replacement battery systems to meet the mechanical performance requirements of electric vehicles. According to the requirements of being waterproof, fire repellent and heat dissipating, Qiu [6] designed a quick-replacement battery box and established its three-dimensional (3D) model. He also used finite-element software to analyze the force of electric vehicles under special working conditions such as sharp braking and sharp turning, as well as to carry out a modal analysis of the quick-replacement battery box. Li et al. [7] used the finite-element method to analyze the mechanical and constraint modes and perform frequency response and vibration tests on a quick-replacement battery box for electric buses. Through the analysis, they obtained the distribution of the weak spots, failure modes and failure-strengthening test conditions of the battery box. Tang [8] established a 3D model of a battery box and its quick-replacement connector, and optimized the structure and lightweight design of the battery box based on the results. Hou [9] established a 3D model of a battery box, and analyzed the static and mode of the quick-replacement battery box structure by using finite-element software. According to the static and heat dissipation simulation results, the structure of the battery box was optimized and improved, increasing its strength and natural frequency. Li et al. [10] analyzed the static and mode characteristics of a quick-replacement battery box for electric vehicles under the conditions of sharp braking and sharp turning, and optimized the structure of the quick-replacement battery box. After optimization design, the quick-replacement battery box was found to not resonate with electric vehicles. According to the above literature analysis, it was found that the current research on the quick-replacement battery boxes for electric vehicles has mainly focused on statics, mode analysis and lightweight aspects. Although the random vibration fatigue of the quick-replacement battery box was analyzed in [11], only a single direction was considered, and no further optimizations were analyzed. These results of the finite-element simulation analysis were verified by a random vibration test system, as pointed out in [11].

Regarding the above problems, a 3D model of the quick-replacement battery box structure for electric vehicles is established in this paper. On this basis, OptiStruct software was used for sweep frequency and random vibration analyses in the three directions of the quick-replacement battery box, and then Ncode software was used to analyze the vibration fatigue. Finally, the structure was optimized according to the analysis results and the lightweight target, resulting in the quick-replacement battery box to fall more in line with the design requirements.

## 2. Quick-Replacement Battery Box Design and Modelling

### *2.1. Quick-Replacement Battery Box Design*

The on-board battery box design aimed to meet the target requirements for stiffness, strength and safety, while also considering the necessary working conditions. A quick-replacement battery box should be easily removable and installable, conforming to the vehicle layout in terms of its external size and shape, and allowing for a quick removal from the chassis. Further, the quick-replacement battery box structure needs to have good vibration resistance and stability, unlike traditional battery boxes that can be arranged on the chassis. To meet the requirements for the quick replacement and strength of the battery box, this paper has selected a rectangular shape that is relatively regular and made from a DC01 steel sheet metal stamping. The basic material parameters of the quick-replacement battery box are shown in Table 1.

**Table 1.** Basic material parameters of the quick-replacement battery box.

| Material | Density (g/mm$^3$) | Poisson's Ratio | Elasticity Modulus (Mpa) | Yield Limit (Mpa) | Anti-Pull Limit (Mpa) |
|---|---|---|---|---|---|
| DC01 | $7.850 \times 10^{-9}$ | 0.3 | $2.07 \times 10^5$ | 195 | 340 |

Following the principle of volume minimizing, and considering the battery life requirements of electric vehicles as well as single-battery specifications, the quick-replacement battery box was made to measure 960 mm × 870 mm × 150 mm.

### 2.2. Three-Dimensional Modeling of the Quick-Replacement Battery Box

According to the design of the quick-replacement battery box, a 3D model was established using SolidWorks software, as shown in Figure 1.

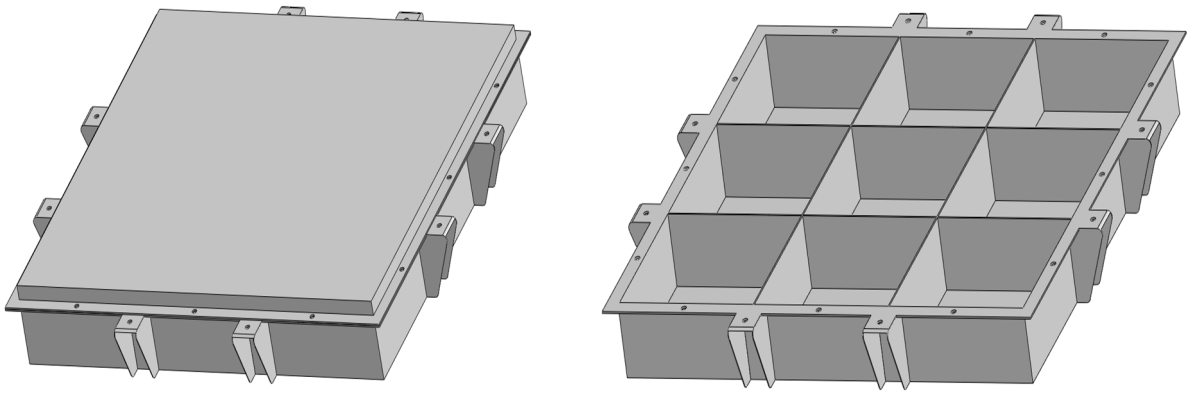

(**a**) (**b**)

**Figure 1.** Quick-replacement battery box 3D model. (**a**) Quick-replacement battery box assembly; (**b**) the lower component of the quick-replacement battery box.

### 2.3. Finite-Element Modeling of the Quick-Replacement Battery Box

The quick-replacement battery box 3D model was imported into HyperMesh; it was made of 3 mm thick sheet metal stamping, which can be treated as a sheet material, with the middle surface extracted and the thickness value added based on the finite-element analysis theory. To ensure the accuracy of the finite-element analysis while taking into account the analysis speed, a 5 mm grid size was selected for the finite-element grid to divide the quick-replacement battery box model. The number of grids was 122,177 and the number of nodes was 123,177. The rigid bar element 2 (RBE2) was used to simulate the bolt connection between the top cover and the lower box, and the finite-element modeling of the quick-replacement battery box is shown in Figure 2.

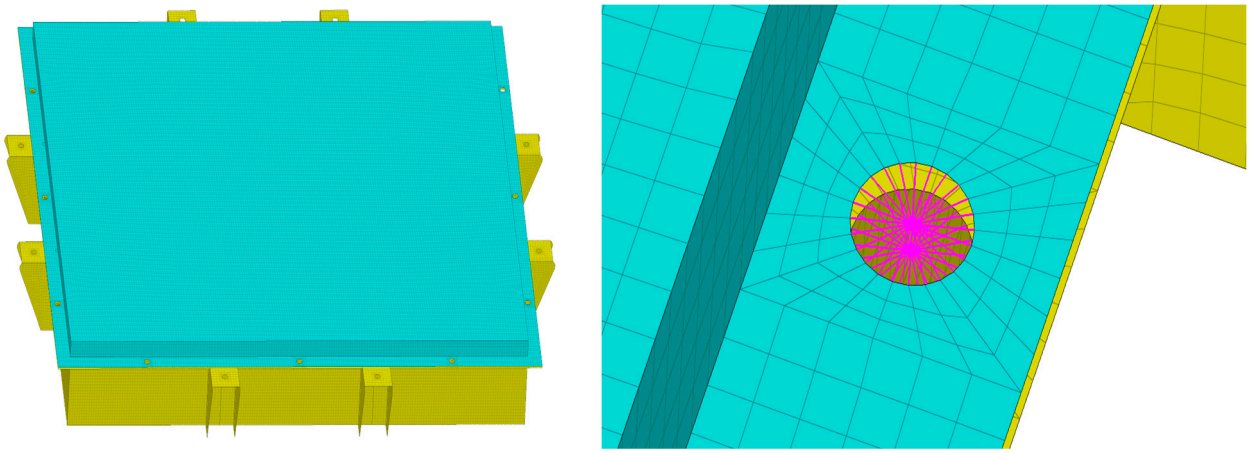

(**a**) (**b**)

**Figure 2.** Finite-element modeling of the quick-replacement battery box. (**a**) Quick-replacement battery box grid division; (**b**) bolted connection.

### 2.4. Boundary Condition Setting

There were several hanging ears on the installation bracket of the quick-replacement battery box. The installation bracket is connected to the bottom plate for electric vehicles and the quick-replacement battery box is installed underneath. The quick-replacement battery box may thus be subject to accidental external impacts and continuous random vibrations from the road, which are mostly transmitted through a bracket mounted on the quick-replacement battery box. To simulate this process, the bolt holes connecting the eight mounting brackets on the lower component of the quick-replacement battery box were rigidly connected through the RBE2 in the finite-element software, a single-point constraint (SPC) as a bench test boundary condition was created at the main node of this RBE2 and a load was applied at this point for further analysis.

### 2.5. Vibration Fatigue Analysis Theory [12]

The random vibration fatigue analysis in this paper was based on the random vibration analysis. During the random vibration fatigue analysis, the power spectral moment of inertia was used to calculate the zero-crossing number and peak-crossing number and construct the probability density function. The moment of inertia, $m_n$, of the $n$-order power spectrum is shown in Equation (1).

$$m_n = \sum_{k=1}^{N} f_k^n G(f_k) \delta f \tag{1}$$

where $f_k$ is the frequency value; $G(f_k)$ is the power spectral density (PSD) response value at frequency $f_k$; and $G(f_k)\delta f$ represents the area of the frequency segment $\delta f$ under the PSD curve at frequency $f_k$.

For any stress amplitude, $\sigma_a^i$, the number of cycles, $N_i$, in any time period, $T$, is shown in Equation (2).

$$N_i = P(\sigma_a^i) N_T \tag{2}$$

For this stress amplitude, the corresponding lifetime, $n_i$, that can be calculated from a given S–N curve and the damage generated at this stress amplitude in any time period, $T$, are shown in Equation (3).

$$D_i = \frac{N_i}{n_i} \tag{3}$$

The total damage caused by the total stress amplitude in any time period, $T$, is shown in Equation (4).

$$D = \sum D_{\mathrm{i}} \tag{4}$$

## 3. Sweep Frequency and Random Vibration Analyses

According to GB/T31467.3-2015 [13], to ensure the safety of on-board batteries when in use, it is necessary to install the on-board battery box on a vibration platform for testing. Vibration testing can be divided into the sweep frequency vibration and random vibration tests. The following simulation was conducted using OptiStruct 2022 software.

### 3.1. Sweep Frequency Vibration Analysis

Based on GB/T31467.3-2015, OptiStruct software was used for a sweep frequency vibration analysis of the quick-replacement battery box in the X-, Y- and Z-directions.

#### 3.1.1. X-Direction Sweep Frequency Vibration Analysis Results

The pre-processed model was solved in accordance with the vibration frequency requirements set in the OptiStruct software. The stress and displacement of the quick-replacement battery box are shown in Figure 3, as determined through the sweep frequency vibration analysis in the X-direction.

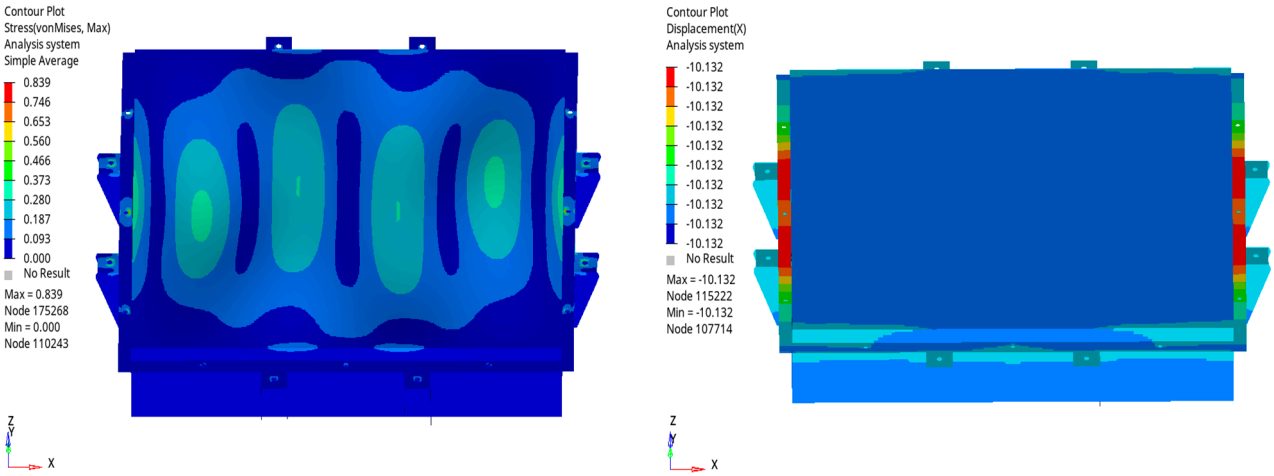


(**a**) (**b**)

**Figure 3.** The stress and displacement of the quick-replacement battery box in the X-direction sweep frequency vibration analysis. (**a**) Maximum stress cloud map; (**b**) displacement cloud map.

The stress and displacement values of the quick-replacement battery box are minimal in the X-direction sweep frequency vibration analysis due to its flat geometry. The maximum stress on the quick-replacement battery box was 0.839 Mpa, with stress concentrated at the top cover and bottom plate. The maximum and minimum displacement values of the quick-replacement battery box were −10.132 mm, indicating that its overall structure in the X-direction remained stable without deformation during vibration.

### 3.1.2. Y-Direction Sweep Frequency Vibration Analysis Results

The pre-processed model was solved in accordance with the vibration frequency requirements set in the OptiStruct software. The stress and displacement of the quick-replacement battery box are shown in Figure 4, as determined through the sweep frequency vibration analysis in the Y-direction.

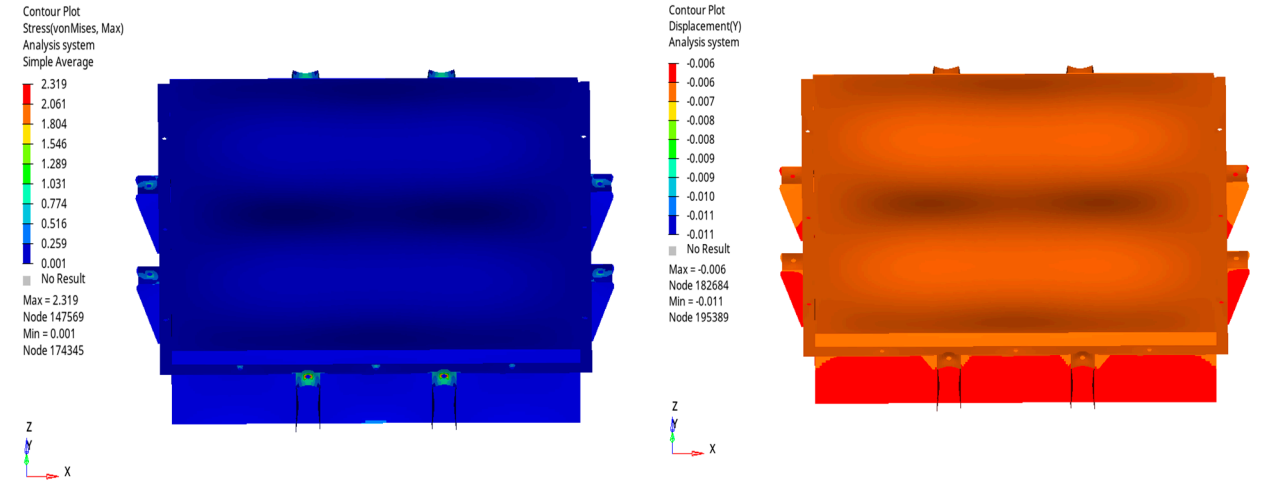


(**a**) (**b**)

**Figure 4.** The stress and displacement of the quick-replacement battery box in the Y-direction sweep frequency vibration analysis. (**a**) Maximum stress cloud map; (**b**) displacement cloud map.

Similar to the X-direction sweep frequency vibration analysis, the stress and displacement values of the quick-replacement battery box were also minimal in the Y-direction

sweep frequency vibration analysis due to its flat geometry. The maximum stress on the quick-replacement battery box was 2.319 Mpa, with stress concentrated also at the top cover and bottom plate. The maximum displacement was −0.006 mm, while the minimum displacement was −0.011 mm, resulting in a difference of 0.005 mm. This means that the overall structure of the quick-replacement battery box had a maximum deviation of 0.005 mm in the Y-direction and exhibited a small vibration amplitude.

#### 3.1.3. Z-Direction Sweep Frequency Vibration Analysis Results

The pre-processed model was solved in accordance with the vibration frequency requirements set in the OptiStruct software. The stress and displacement of the quick-replacement battery box are shown in Figure 5, as determined through the sweep frequency vibration analysis in the Z-direction.

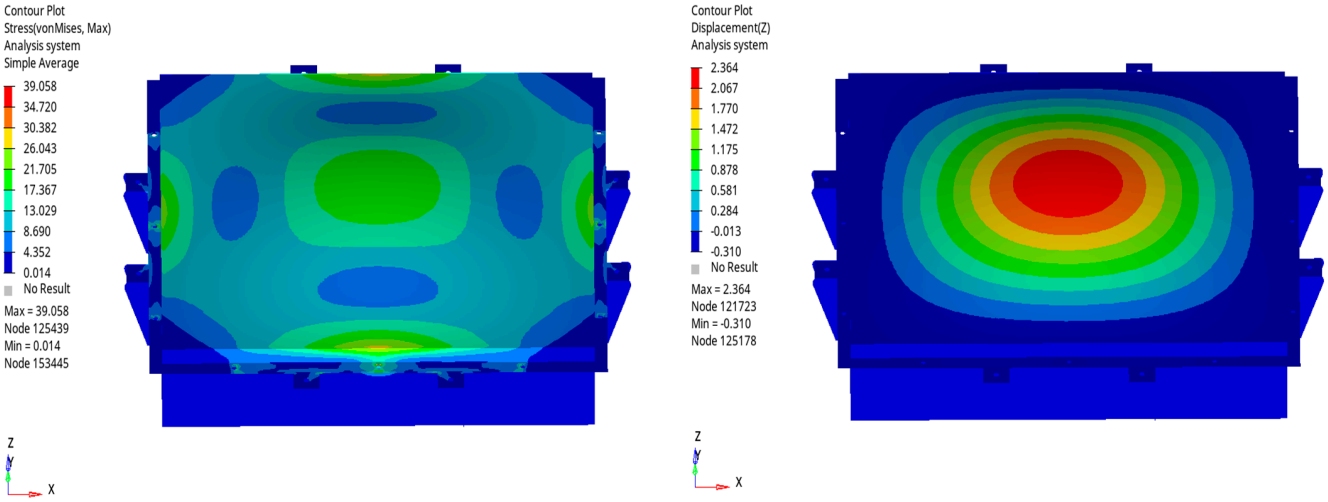


(**a**) (**b**)

**Figure 5.** The stress and displacement of the quick-replacement battery box in the Z-direction sweep frequency vibration analysis. (**a**) Maximum stress cloud map; (**b**) displacement cloud map.

As seen in Figure 5, the maximum stress on the quick-replacement battery box is 39.058 Mpa, and the maximum stress values occur at the bolt and the edge of the top cover, with large stresses also appearing in the center of the top cover and the bottom plate. Additionally, stress concentration phenomena were observed in multiple locations. The quick-replacement battery box had a maximum displacement of 2.364 mm and a minimum displacement of −0.310 mm. This means that the overall structure of the quick-replacement battery box had a maximum deviation of 2.674 mm in the Z-direction and also exhibited a small vibration amplitude.

According to the results of the sweep frequency vibration analysis in three directions, the maximum stress on the quick-replacement battery box was 39.058 Mpa, which is significantly lower than the allowable stress for the DC01 material. This indicates that the structure of the quick-replacement battery box met the allowable stress requirements for the selected material with a large margin. Therefore, the lightweight design can be considered for optimization.

### *3.2. Random Vibration Analysis*

To simulate the vibration load to which the quick-replacement battery box may be subjected due to an accidental external impact and continuous random road vibrations, we conducted a random vibration test in the X-, Y- and Z-directions using the OptiStruct software. This allowed us to obtain equivalent stress root-mean-square (RMS) cloud maps

in these three directions under 1$\sigma$, following the safety requirements and the test method specified by GB/T31467.3-2015.

The equivalent stress RMS cloud map under 1σ that was obtained in the X-direction random vibration analysis is shown in Figure 6. The maximum equivalent stress RMS occurred at the hanging ear and the X-axis edge of the top cover of the quick-replacement battery box, with a value of 0.112 MPa. The equivalent stress RMS value under 6$\sigma$ was 0.672 MPa, which was significantly lower than the yield strength of the DC01 material at 195 MPa.

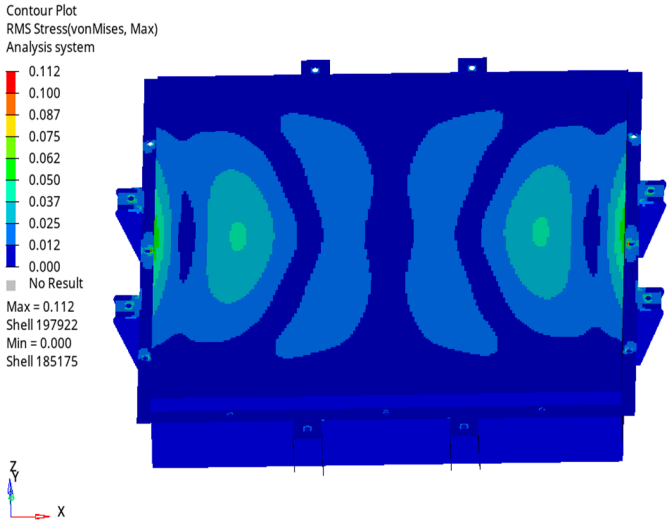


**Figure 6.** The equivalent stress RMS cloud map in the X-direction.

The equivalent stress RMS cloud map under 1σ that was obtained in the Y-direction random vibration analysis is shown in Figure 7. The maximum equivalent stress RMS occurred at the hanging ear and the Y-axis edge of the top cover of the quick-replacement battery box, with a value of 0.083 MPa. The equivalent stress RMS value under 6$\sigma$ was 0.498 MPa, which was significantly lower than the yield strength of the DC01 material at 195 MPa.

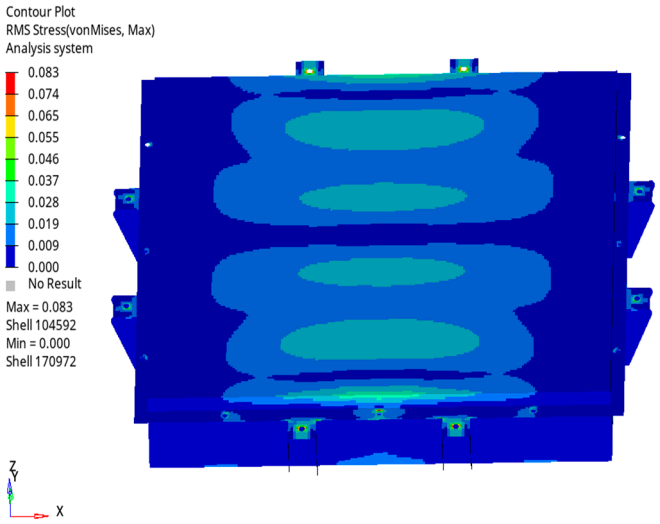


**Figure 7.** The equivalent stress RMS cloud map in the Y-direction.

The equivalent stress RMS cloud map under 1σ that was obtained in the Z-direction random vibration analysis is shown in Figure 8. The maximum equivalent stress RMS occurred at the hanging ear and the four edges of the top cover of the quick-replacement

battery box, with a value of 13.097 MPa. The equivalent stress RMS value under 6$\sigma$ was 78.582 MPa, which was significantly lower than the yield strength of the DC01 material at 195 MPa.

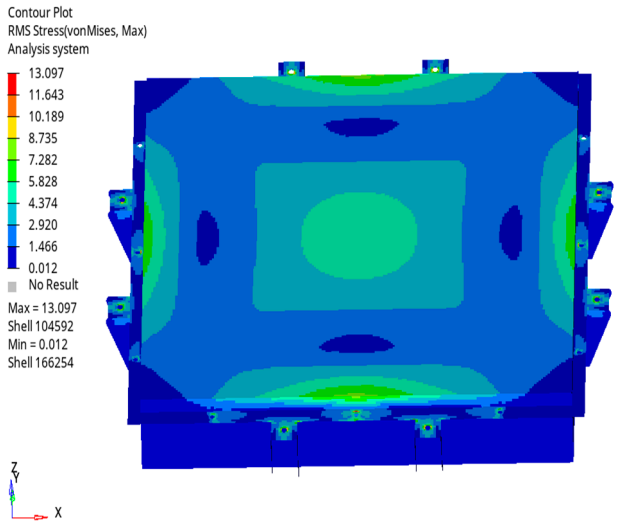


**Figure 8.** The equivalent stress RMS cloud map in the Z-direction.

As seen in Figures 6–8, the equivalent stress RMS of the random vibration in the X-, Y- and Z-directions met the 6$\sigma$ requirement. With a probability of 99.999999985%, there will be no plastic deformations, and the forces acting on the components of the quick-replacement battery box will remain within their elastic range while being lower than the yield strength of the DC01 material at 195 Mpa; that is, there are only 0.002 failures per million experiments, which satisfies the design requirements.

Furthermore, not only can the equivalent stress RMS cloud map be obtained, but the acceleration PSD curve for each point of the quick-replacement battery box can also be obtained through the random vibration analysis using OptiStruct software. Figures 9–11 are the acceleration PSD curves in the X-, Y- and Z-directions, respectively, in the X-direction random vibration analysis on the bottom plate of the quick-replacement battery box. These acceleration PSD curves are essential prerequisites for a further random vibration fatigue analysis of the quick-replacement battery box using OptiStruct software.

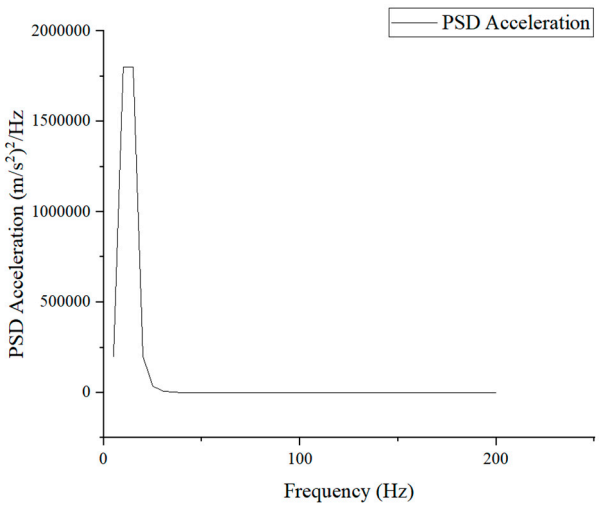


**Figure 9.** PSD curve of X-direction vibration and X-direction acceleration response.

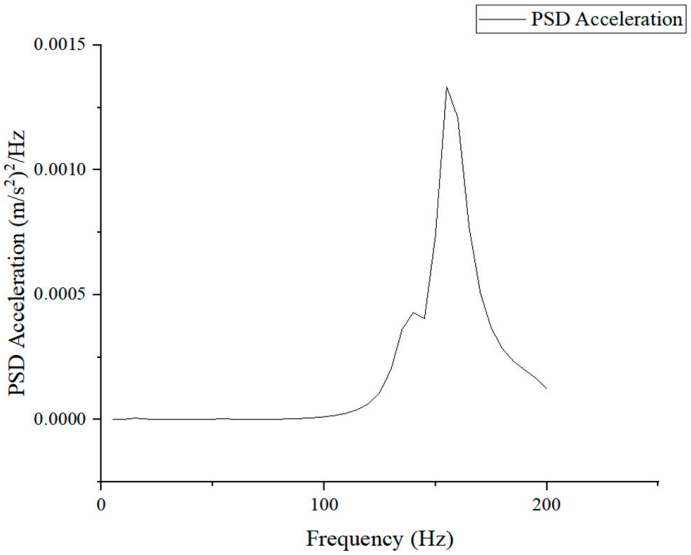


**Figure 10.** PSD curve of X-direction vibration and Y-direction acceleration response.

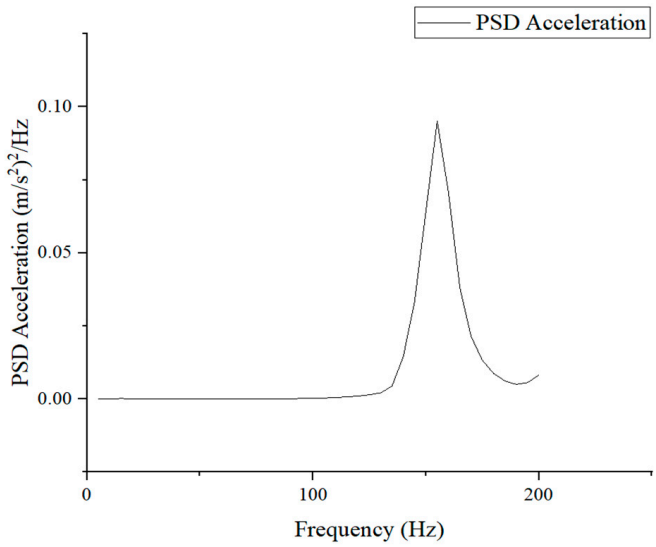


**Figure 11.** PSD curve of X-direction vibration and Z-direction acceleration response.

## 4. Random Vibration Fatigue Analysis

The damage position of the quick-replacement battery box was identified during the random vibration fatigue analysis, which lays the foundation for further optimization design. First, the stress responses of the quick-replacement battery box in three directions were imported into the Ncode software to define the S–N characteristics of the DC01 material. The S–N curve of the DC01 material of the quick-replacement battery box is shown in Figure 12.

Then, according to GB/T31467.3-2015, we input the acceleration PSD spectra of the X-, Y- and Z-directions into the finite-element model of the quick-replacement battery box in the Ncode software as the vibrational load with defined S–N properties of the DC01 material, and set the number of cycles to 75,600 (with the characterized vibration time of 21 h). Then, the random vibration process of the quick-replacement battery box was initiated and the cloud maps of random vibration fatigue damage and life were obtained, as shown in Figures 13 and 14.

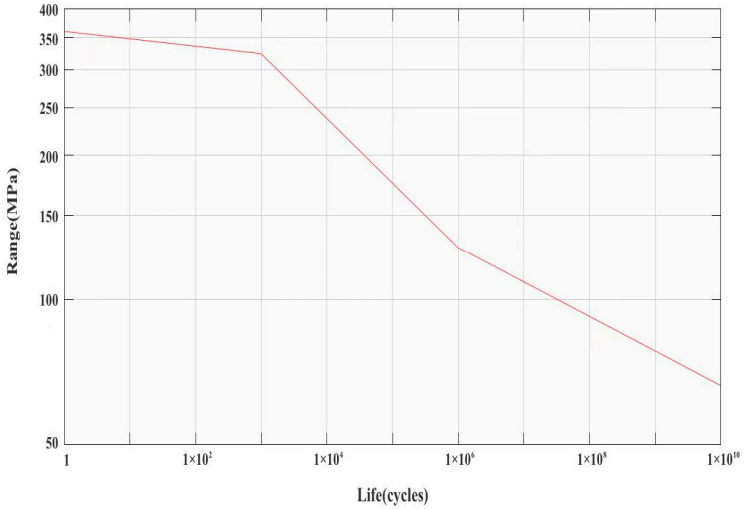


**Figure 12.** The S–N curve of the DC01 material of the quick-replacement battery box.

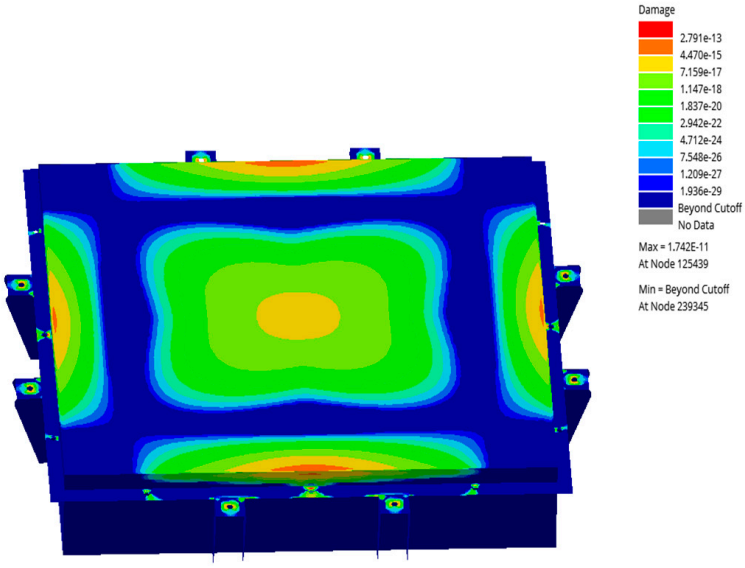


**Figure 13.** The random vibration fatigue damage cloud map of the quick-replacement battery box.

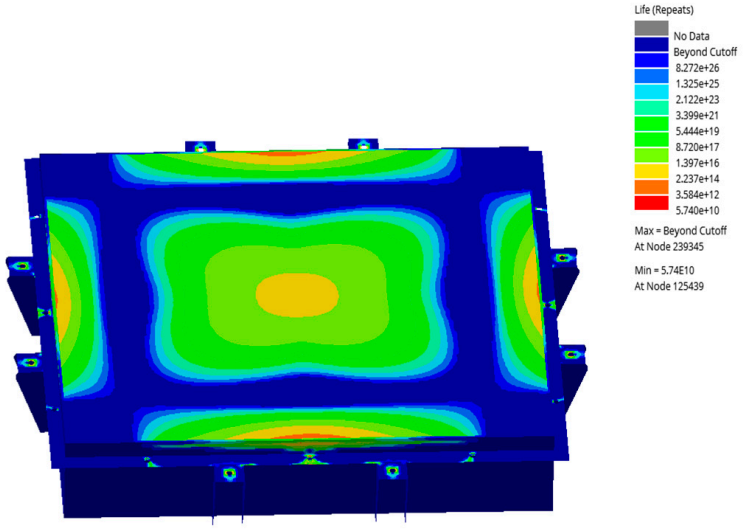


**Figure 14.** The random vibration fatigue life cloud map of the quick-replacement battery box.

As seen in Figures 13 and 14, the most dangerous position was located at the bolt installed in the quick-replacement battery box, and its minimum fatigue life was $5.740 \times 10^{10}$; that is, the structure of the quick-replacement battery box can meet the fatigue requirements under random vibration conditions, indicating that it can fulfill the fatigue life requirements in changeable operating environments and driving conditions, safeguarding the battery pack and ensuring electric vehicle safety.

## 5. Quick-Replacement Battery Box Optimization Design

### *5.1. Quick-Replacement Battery Box Structure after Optimization Design*

According to the vibration and vibration fatigue analyses, the maximum stress of the quick-replacement battery box was 39.058 Mpa, which is significantly lower than the allowable stress of the DC01 material at 150 MPa. Therefore, the structure of the quick-replacement battery box is sufficiently strong considering that it is a lightweight design. The thickness of the quick-replacement battery box was 3 mm, and it should not be made thinner; therefore, punching the box body to meet the lightweight requirements was considered. According to the above analysis, it can be concluded that the battery baffle in the internal structure of the lower compartment of the quick-replacement battery box experienced less stress during vibration. Therefore, it was decided that holes should be added to the baffle. The internal structure of the lower box before and after optimization is shown in Figure 15. The weight of the quick-replacement battery box was reduced by approximately 4 kg due to the drilled holes.

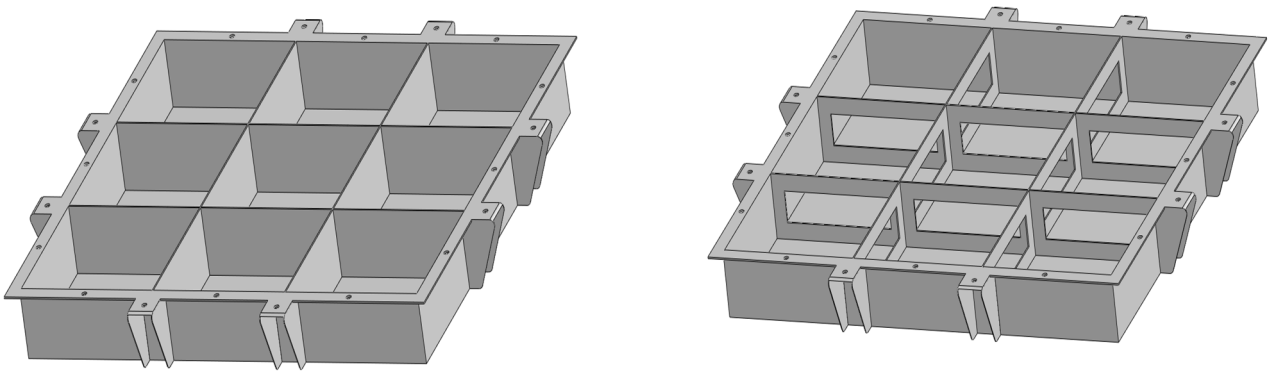

(**a**) (**b**)

**Figure 15.** (**a**) Internal structure of the lower box before optimization; (**b**) internal structure of the lower box after optimization.

Additionally, the stress on the quick-replacement battery box during the vibration analysis was small. However, there was some stress concentrated at the top cover and bottom plate of the quick-replacement battery box, which can cause damage after prolonged use. Therefore, reinforcement ribs were designed in these parts to reduce the stress concentration, and also to help inhibit the deformation of the quick-replacement battery box. The position of the reinforcement ribs is shown in Figure 16.

The 3D model of the quick-replacement battery box after optimization is shown in Figure 17.

### *5.2. Sweep Frequency and Random Vibration Analysis of the Quick-Replacement Battery Box after Optimization Design*

Based on GB/T31467.3-2015, OptiStruct software was used for the sweep frequency vibration analysis of the quick-replacement battery box in the X-, Y- and Z-directions, and the analysis results were compared with those obtained before optimization. The results of the sweep frequency vibration analysis in the X-, Y- and Z-directions are shown in Figures 18–20.

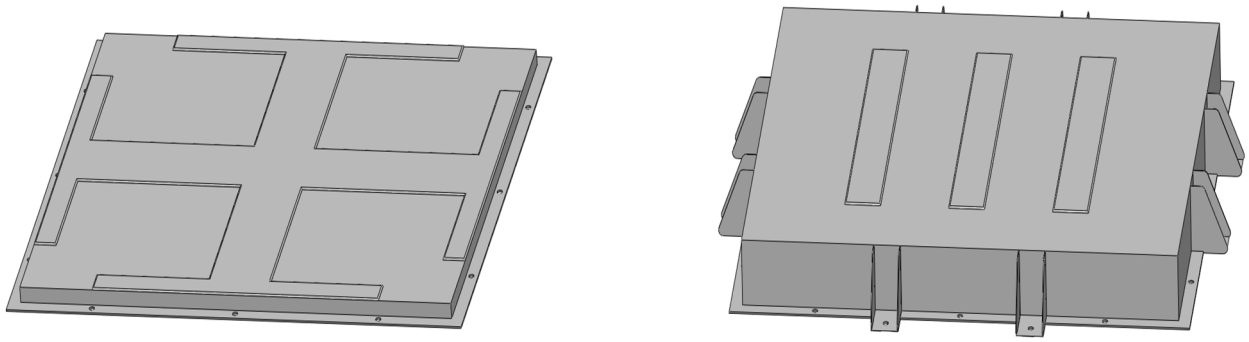

(**a**) (**b**)

**Figure 16.** The reinforcement ribs of the quick-replacement battery box after optimization. (**a**) Reinforcement ribs of the top cover; (**b**) reinforcement ribs of the lower box.

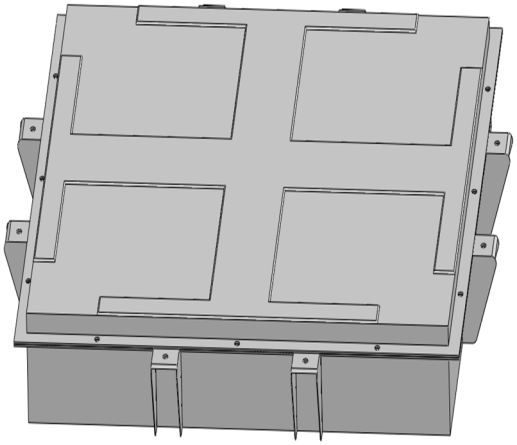

**Figure 17.** The 3D model of the quick-replacement battery box after optimization.

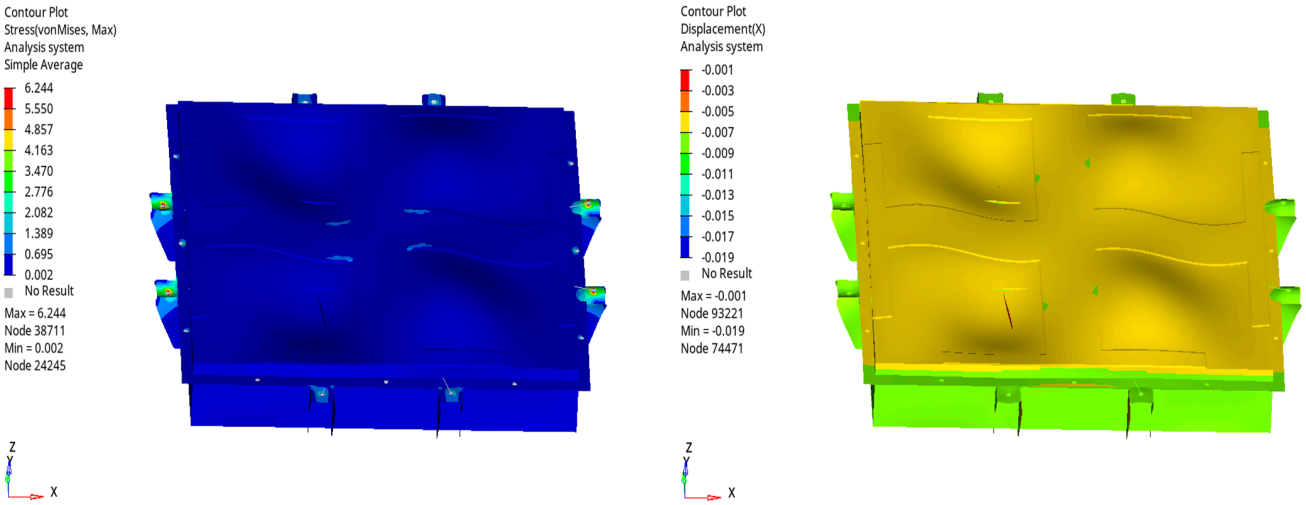


(**a**) (**b**)

**Figure 18.** The stress and displacement of the quick-replacement battery box after optimization as determined with the X-direction sweep frequency vibration analysis. (**a**) Maximum stress cloud map; (**b**) displacement cloud map.

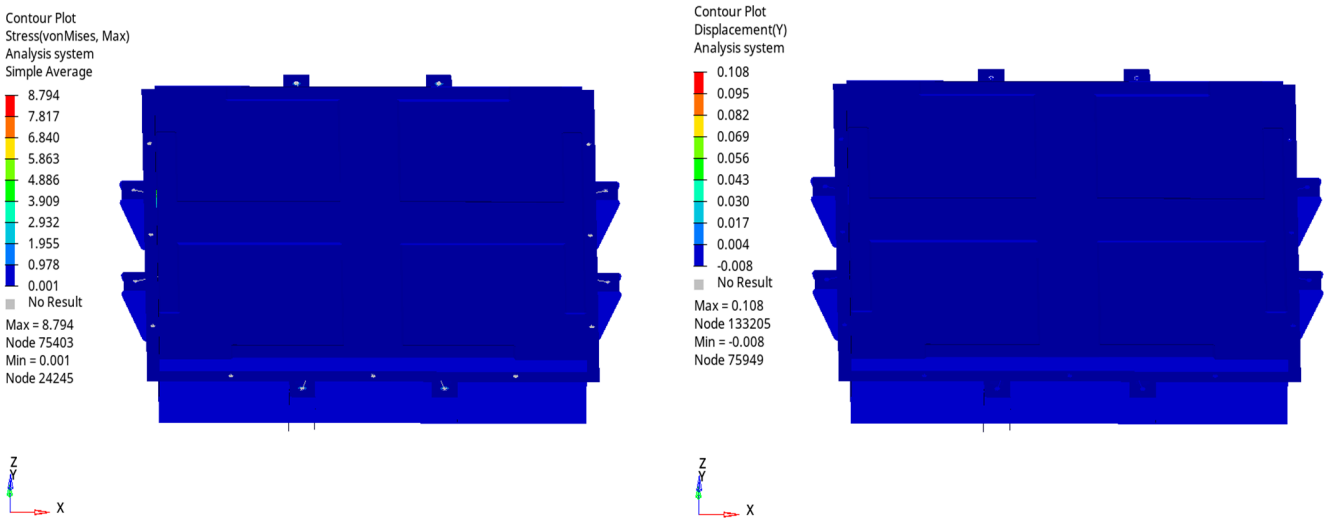


(**a**) (**b**)

**Figure 19.** The stress and displacement of the quick-replacement battery box after optimization as determined with the Y-direction sweep frequency vibration analysis. (**a**) Maximum stress cloud map; (**b**) displacement cloud map.

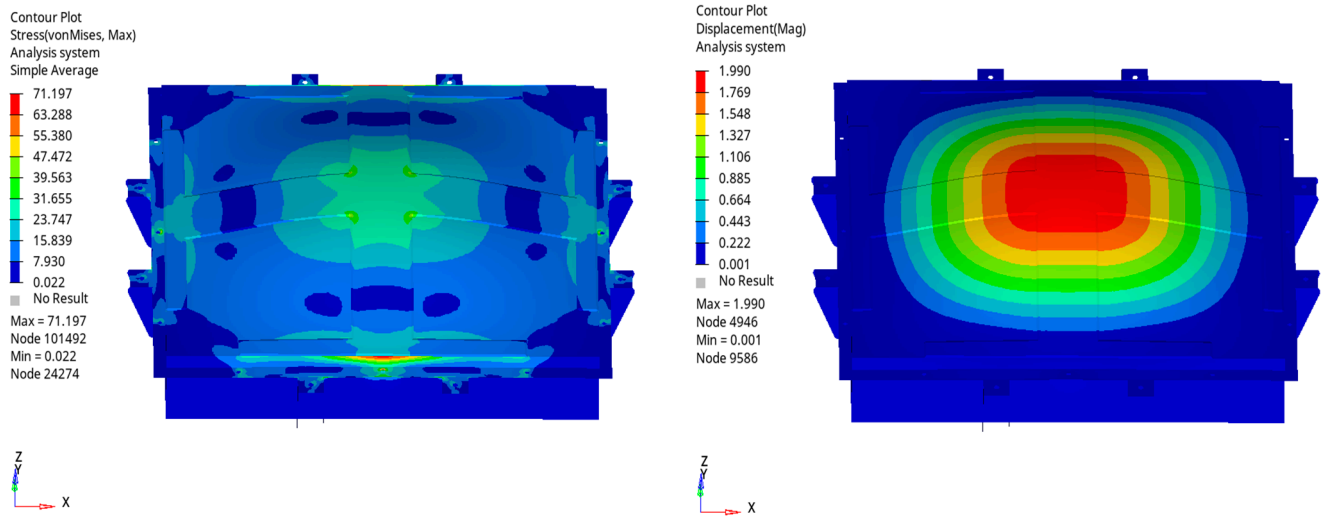


(**a**) (**b**)

**Figure 20.** The stress and displacement of the quick-replacement battery box after optimization as determined with the Z-direction sweep frequency vibration analysis. (**a**) Maximum stress cloud map; (**b**) displacement cloud map.

As seen in Figures 18–20, the optimized quick-replacement battery box still experienced maximum stress during sweep frequency vibration analysis, with a value of 71.197 Mpa at both the top cover and inside the quick-replacement battery box. Additionally, relatively high stress was also measured at the top cover and the bottom center of the quick-replacement battery box. The optimized quick-replacement battery box had a maximum deformation of 1.989 mm at its top cover and bottom center.

The results of the vibration analysis of the quick-replacement battery box before and after optimization were compared and Table 2 shows the maximum stress and deformation during sweep frequency vibration analysis, both before and after optimization.

**Table 2.** Comparison of maximum stress and deformation during sweep frequency vibration analysis, both before and after optimization.

| | Maximum Stress (Mpa) | Maximum Deformation (mm) |
|---|---|---|
| Before optimization | 39.058 | 2.674 |
| After optimization | 71.197 | 1.989 |

After optimization design, the maximum stress of the quick-replacement battery box increased by 32.139 MPa, while the maximum deformation decreased from 2.674 mm to 1.989 mm. Although there was an increase in stress after optimization, the maximum stress remained below the allowable stress of the DC01 material at 150 MPa. The structural strength met the requirements and the optimized design reduced the overall weight of the quick-replacement battery box by 4 kg, achieving the lightweight goal.

### *5.3. Random Vibration Fatigue Analysis of the Quick-Replacement Battery Box after Optimization Design*

After conducting the same random vibration fatigue analysis on the optimized design as that carried out before optimization, the cloud maps of random vibration fatigue damage and life were obtained and are shown in Figures 21 and 22.

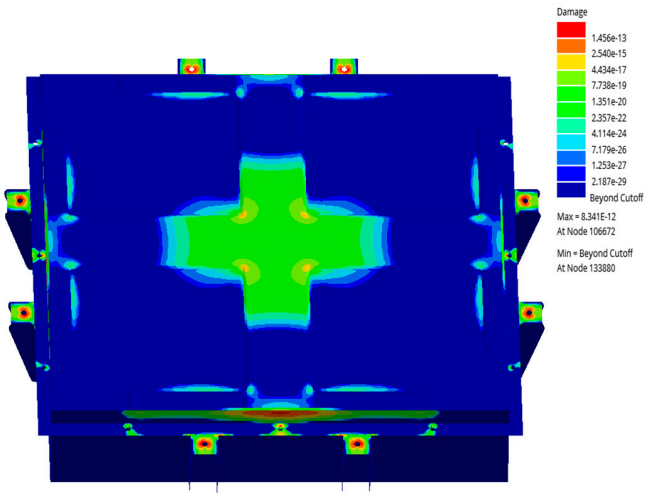


**Figure 21.** The random vibration fatigue damage cloud map of the quick-replacement battery box after optimization.

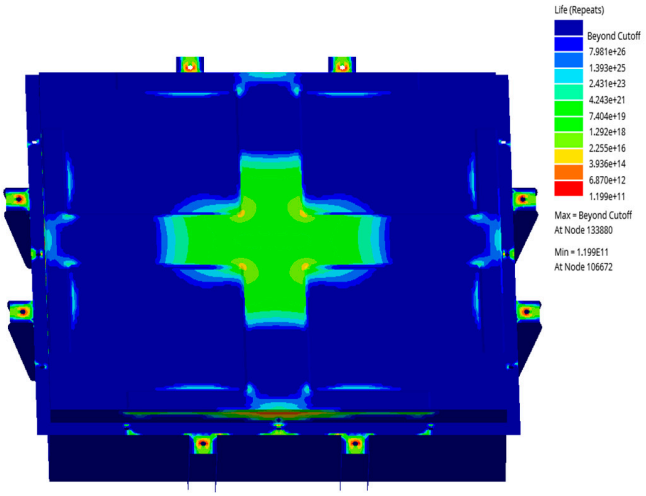


**Figure 22.** The random vibration fatigue life cloud map of the quick-replacement battery box after optimization.

The analysis results show that the optimized quick-replacement battery box had a minimum fatigue life of $1.199 \times 10^{11}$, as determined in the random vibration fatigue analysis; that is, it still met the fatigue requirements while being reduced by 4 kg compared to the weight of the pre-optimized battery box. Therefore, optimizing the quick-replacement battery box is feasible and necessary.

## 6. Conclusions

This paper established a CAD model and finite-element model for electric vehicles. Based on these models, OptiStruct software was used to perform sweep frequency and random vibration analyses of the quick-replacement battery box, while Ncode software was used to analyze the random vibration fatigue. Finally, the structure of the quick-replacement battery box was optimized according to the analysis results and lightweight targets in order to meet the design requirements.

(1) After the sweep frequency vibration analysis before design optimization, the maximum stress was 39.058 MPa, which is much lower than the allowable stress of the DC01 material at 150 MPa. The equivalent stress RMS value under $6\sigma$ as found in the random vibration analysis was 78.582 MPa, which was significantly lower than the allowable stress of the DC01 material at 150 MPa. In other words, the results of the random vibration analysis met the requirement of $6\sigma$, with only 0.002 failures per one million experiments. Additionally, the minimum fatigue life of the quick-replacement battery box as identified in the random vibration fatigue analysis was $5.740 \times 10^{10}$, indicating that it met the requirements for fatigue life under random vibration conditions.

(2) After optimizing the design, the maximum stress of the quick-replacement battery box increased to 71.197 Mpa, as determined in the sweep frequency vibration analysis, but was still less than the allowable stress of the DC01 material at 150 MPa. The random vibration fatigue analysis showed that the minimum fatigue life of the optimized quick-replacement battery box was $1.199 \times 10^{11}$. From a lightweight perspective, there was a reduction in total mass of about 4 kg for the quick-replacement battery box after optimization. Therefore, after optimization, the structure of the quick-replacement battery box met the design requirements.

(3) According to the results of the vibration and fatigue analysis, the Z-direction was where the quick-replacement battery box was most susceptible to maximum damage. Therefore, further studies should focus on analyzing vibrations in the vertical direction more closely. Furthermore, it is crucial to strengthen the structural strength of vulnerable parts, such as that of each connection and the thin plate center of the quick-replacement battery box.

**Author Contributions:** J.L.: writing—review and editing, methodology, investigation, and formal analysis. G.H.: modeling, data curation and analysis. J.C.: supervision and conceptualization. All authors have read and agreed to the published version of the manuscript.

**Funding:** This research was funded by the financial support of the Ministry of Education's Collaborative Education Project, grant number 220603950174204; the Guangdong University Student Climbing Program, grant number pdjh2022b0554; and the Innovation and Entrepreneurship Projects for College Students, grant number 202210580009.

**Data Availability Statement:** Not applicable.

**Conflicts of Interest:** The authors declare no potential conflict of interest concerning the research, authorship and/or publication of this article.

## References


1. Fan, Y. Research on the Enterprise Level of New Energy Vehicles' Development Strategy. Master's Thesis, Nanchang University, Nanchang, China, 2014.
2. Zhang, H.; Tang, W.W.; Zhang, N.; Zhang, W.G. Mobile battery-swapping service for electric vehicles. *Power Syst. Clean Energy* **2016**, *32*, 142–145.
3. Wang, X.R. Analysis of the development, current research status and challenges of battery exchange modes for electric vehicles. *J. Sichuan Vocat. Tech. Coll.* **2021**, *31*, 163–168.
4. Lu, Z.Y.; Zong, Y.Y.; Zhao, M.Y.; Zhang, H. Modal analysis and optimization of electric vehicle's fast-swap battery box. *Appl. Mech. Mater.* **2013**, *241*, 1992–1999. [CrossRef]
5. Wang, W.N.; Li, B.; Wang, Y. Design of battery fast-swap system for electric vehicle. *Appl. Mech. Mater.* **2014**, *628*, 190–194. [CrossRef]
6. Qiu, C. The Research on Stowing of Fest-Exchange Battery Pack of Electric Vehicles. Master's Thesis, Lanzhou University of Technology, Lanzhou, China, 2014.
7. Li, S.Y.; Chen, Y.; Jiang, F.C.; Zhao, J.; Wang, G. Research on the finite element analysis and failure strengthening test of electric bus quick-change battery box. In Proceedings of the 2015 8th International Conference on Intelligent Computation Technology and Automation, Nanchang, China, 14–15 June 2015.
8. Tang, G.T. The Swapping Traction Battery Enclosure Structure Optimization and Lightweight Design. Master's Thesis, Chongqing Jiaotong University, Chongqing, China, 2016.
9. Hou, W.N. Research on Structure and Thermal Performance for Fast-Exchange Battery Box of Electric Vehicle. Master's Thesis, Chang'an University, Xi'an, China, 2018.
10. Li, J.Y.; Lu, Z.D. Finite element analysis and optimization design of electric vehicle quick replacement battery box. *Mod. Manuf. Eng.* **2020**, *7*, 31–38.
11. Xu, Y.J.; Yang, L.; Lan, Z.B. Study on the fatigue characteristics of quick-change battery box in electric passenger car. *Machinery* **2023**, *61*, 1–6.
12. Liu, Y.; Chen, B.; Luo, F. *OptiStruct Structure Analysis and Engineering Application*; Machinery Industry Press: Beijing, China, 2021; pp. 327–328, 330.
13. *GB/T 31467.3-2015*; Lithium Ion Power Battery Packs and Systems for Electric Vehicles-Part 3: Safety Requirements and Test Methods. China Standards Press: Beijing, China, 2015.


**Disclaimer/Publisher's Note:** The statements, opinions and data contained in all publications are solely those of the individual author(s) and contributor(s) and not of MDPI and/or the editor(s). MDPI and/or the editor(s) disclaim responsibility for any injury to people or property resulting from any ideas, methods, instructions or products referred to in the content.